Materials Horizons

ROYAL SOCIETY OF CHEMISTRY

COMMUNICATION

View Article Online
View Journal | View Issue

Cite this: *Mater. Horiz.*, 2025, 12, 802

Received 18th June 2024,
Accepted 15th October 2024

DOI: 10.1039/d4mh00780h

rsc.li/materials-horizons

Chemically robust functionalized covalent organic framework for the highly efficient and selective separation of bromine†

Sahel Fajal, [a] Dipayan Ghosh, [a] Kishalay Biswas, [a] Writakshi Mandal, [a] Nayan Sarkar, [a] Gourab K. Dam, [a] Anirban Roy, [a] Antak Roychowdhury, [a] Dipanjan Majumder, [a] Rajashri R. Urkude, [b] Mandar M. Shirolkar [cd] and Sujit K. Ghosh *[ae]

Effective sequestration of bromine holds great promise for the chemical industry's safe expansion, environmental preservation, and public health. However, attaining this goal is still challenging due to the serious drawbacks of existing adsorbents such as limited capacity, low retention efficiency, and sluggish uptake kinetics. Herein, we report a strategy-driven systematic study aimed at significantly enhancing multiple host–guest interactions to obtain functionalized covalent-organic frameworks for the efficient sequestration of bromine. Results showed that the presence of specific quantities of selective binding sites of the porous frameworks afford stronger host–guest interactions and therefore higher bromine adsorption capacities. The developed framework exhibits high bromine sorption capacity of up to 5.16 g g^{-1} in the vapor phase and 8.79 g g^{-1} in the aqueous phase under static adsorption conditions with fast kinetics, large distribution coefficient (K_d ~10^5 mL g^{-1}), high retention efficiency and reusability. Moreover, the adsorbent is able to sequestrate trace bromine (from 13 ppm to below 4 ppm) from aqueous medium with fast adsorption kinetics (86.3% within less than 3 h) and demonstrates the selective extraction of bromine over iodine under both static and dynamic conditions. These results were further utilized to demonstrate recycling-selective and highly efficient bromine capture from a real-water system, exhibiting excellent scalability and affordability, as exemplified using COF membranes in a continuous flow-through process.

New concepts

Due to its wide range of industrial applications, bromine is a significant resource that is used in various chemical- and energy-related applications. Nevertheless, bromine's severe toxicity, corrosiveness, and volatile nature give rise to serious challenges in its handling, storage, and safe transportation. Although decades of expertise has been applied for minimizing these issues, leaks or explosions continue to cause terrible accidents worldwide. Therefore, it is highly desirable to create novel materials that will enable the safe handling, on-demand distribution, and open-air storage of bromine. Herein, we demonstrated a strategy-driven investigation that aimed to produce a series of skeleton-engineered COFs for the highly effective sequestration of bromine by significantly enhancing various host–guest interactions. Under both static and dynamic adsorption conditions, the adsorbent demonstrated high bromine sorption capacities in the vapor and aqueous phases. The adsorbent showed a preference for the separation of bromine over iodine. Furthermore, a highly effective continuous flow-through method for selectively separating Br_2 under dynamic conditions was established utilizing the COF membranes, thus offering excellent scalability and cost. Our study opens up new horizons to address the long-standing problems associated with halogen separation and provides both fundamental and practical insights into the function of framework-integrated adsorption sites in bromine capture.

Introduction

Bromine is a valuable resource with many commercial uses, including those in flame retardants, pharmaceuticals, drilling fluids, and low-cost energy storage systems (Zn–Br batteries), therefore playing key roles in various chemical and energy industries.[1–4] However, the extreme toxicity, corrosiveness, and volatile nature of bromine significantly hinder its safe storage, handling and transit.[5] The separation of pure bromine from other halogens such as iodine also holds great promise for various chemical processes.[6] When bromine is discharged into air or water, its inhalation exposure can harm humans and other living beings.[7] Elemental bromine as well as its potential secondary pollutants are carcinogenic and mutagenic in water, causing serious water pollution.[8,9] Therefore, although disadvantages such as low adsorption rate, poor retention efficiency, and high volatility

[a] *Department of Chemistry, Indian Institute of Science Education and Research (IISER) Pune, Dr Homi Bhaba Road, Pashan, Pune 411008, India. E-mail: sghosh@iiserpune.ac.in*
[b] *Beamline Development and Application Section Bhabha Atomic Research Centre, Mumbai – 400085, India*
[c] *Advanced Bio-Agro Tech Pvt. Ltd, Baner, Pune 411045, India*
[d] *Norel Nutrient Bio-Agro Tech Pvt. Ltd, Baner, Pune 411045, India*
[e] *Centre for Water Research (CWR), Indian Institute of Science Education and Research (IISER) Pune, Dr Homi Bhabha Road, Pashan, Pune 411008, India*

† Electronic supplementary information (ESI) available. See DOI: https://doi.org/10.1039/d4mh00780h

exist, effective sequestration and separation of bromine are essential for the chemical/battery industry's safe expansion, environmental preservation, and public health.

Adsorption-based sequestration processes using porous materials are found to be more effective over traditional techniques used to capture bromine from contaminated systems owing to their easy working principle, low maintenance cost and lack of corrosive medium requirement.[5,6] Considering this, to date, only a few studies have been devoted to developing various porous material-based excellent adsorbents for the sequestration of bromine at room temperature.[5,6,10–13] Among them, metal–organic frameworks,[5,10] porous organic polymers,[6] covalent organic frameworks,[11,12] porous organic cages,[13] and vacancy-ordered perovskites[14] have been investigated for the adsorption of bromine from the vapor phase and organic solvent medium. However, the majority of studies are restricted to investigating their kinetics, uptake capacity, capture at high temperature, retention efficiency and selectivity. This has spurred researchers to develop new materials that can effectively capture bromine. In addition, most of the studies have been focused only on the capture of bromine either from the vapor phase or from organic solvents under static conditions.[15] The extraction of molecular bromine (Br_2) from aqueous media with high uptake capacity and fast kinetics under both static and dynamic conditions has rarely been explored in the literature.[15] This might be due to the less chemical/hydrolytic stability of the developed adsorbents, which restricts their large-scale practical application. Also, studies on the separation of bromine from other halogens such as iodine (I_2) are very limited,[6] and none of these studies have demonstrated sequestration at elevated temperatures. Moreover, the selective uptake of bromine from low-concentration aqueous solutions in the presence of large excesses of other interferences has not been explored yet. Additionally, no studies have been conducted on continuous flow-through-based bromine extraction from water as well as the selective separation of Br_2 under dynamic conditions. There is thus a motivation to develop a highly stable, scalable, and efficient adsorbent for bromine sequestration with large uptake capacity, fast kinetics, high retention efficiency, selectivity, recyclability and capture at different relevant temperatures from both air and water. This area is mostly unexplored due to the lack of a proper adsorbent design strategy.

Understanding how to harness the molecular interactions between bromine and the adsorbent to increase the chemical and physical properties of the active capture sites is crucial for designing an efficient bromine adsorbent. In order to do this, we re-examined the earlier research and looked into the underlying mechanism(s) behind effective bromine uptake. The textural characteristics of porous sorbents such as surface area, pore size, and pore volume are responsible for the high adsorption capacity of bromine.[6,10,13] Furthermore, because a suitable charge-transfer complex is formed by the strong interaction between the electron-deficient bromine molecules and the anticipated dense binding sites of electron-rich porous materials, substantial bromine uptake is favoured.[6,13,16,17] Additionally, a number of single or combined effects of multiple functionalities, including the induction of conjugated frameworks rich in pi electrons, presence of heterocyclic moieties, and incorporation of particular heteroatoms, explicitly contributes to increased bromine capture efficiency.[6,13–18] Also, to hasten significant bromine enrichment, N-doped structural moieties, such as amine, imine, and triazine, have been introduced into aromatic networks among the heterocyclic sites.[13–19] Moreover, aromatic derivatives-based adsorbents with phenolic hydroxyl groups shows the effective sorption of bromine through facile oxidation[6] as well as bromination *via* hydrogen substitution reactions.[15] Consequently, a material must demonstrate the combined impacts of the numerous aforementioned criteria in order to be an ideal bromine adsorbent. On the other hand, fabricating a successful bromine adsorbent requires striking an appropriate balance between these variables. This is especially true when adding more binding sites to adsorbents as this typically compromises the surface characteristics.[16] As an example, a hypothetically high degree of phenolic hydroxyl groups can be introduced into an adsorbent to increase its interaction with bromine while concurrently decreasing its porosity. This outcome further reduces the ability to collect bromine. The essential task in this situation is to create an efficient bromine adsorbent by adding the right proportion of active binding sites to a highly stable material while preserving its porosity.

Covalent organic frameworks (COFs) are crystalline porous polymers with ordered nanoscale pores constructed *via* the robust covalent bonding of lightweight organic building units.[20] The regular porous architecture along with the diverse functional tunability of COFs have attracted significant research attention in the context of gas adsorption or separation, heterogeneous catalysis, pollutants sequestration, sensing, electrochemical application, and many more.[21–23] Recently, due to their combined unique characteristics, keto–enol-based imine-functionalized COFs have gained recognition as promising materials for a range of cutting-edge applications, including adsorption, separation, electro/photocatalyst, and environmental remediation due to their favorable high chemical stabilities.[24–27] Notably, these COFs can be functionalized with requisite adsorption active sites through the selection of suitable monomers, resulting in high bromine adsorption capacity. Additional versatility for functionality engineering is provided by the β-ketoenamine COFs, which are prepared with hydroxyl monomers and triazine groups to insert the desired functionality into the robust imine COF structure for targeted bromine capture application.[27–29] Although these COFs have been used for various applications, to the best of our knowledge, they have yet to be tested for bromine capture. Moreover, the easy and facile fabrication of the thin film-based membranes of these COFs allows the swift and efficient dynamic separation of the targeted analytes from contaminated systems.[30–32]

On the account of the above considerations, herein, we demonstrate a strategy-driven systematic study aimed at significantly enhancing multiple host–guest interactions to obtain a series of skeleton-engineered COFs for the efficient sequestration of bromine. Results showed that the presence of specific quantities of selective binding sites of the frameworks afford stronger host–guest interactions and therefore higher bromine

adsorption capacities. Among all the developed frameworks, the best-performing one exhibits bromine sorption capacity of up to 5.16 g g^{-1} in the vapor phase and 8.79 g g^{-1} in the aqueous phase under static adsorption conditions with fast kinetics, large distribution coefficient (K_d $\sim 10^5$ mL g^{-1}), high retention efficiency and decent reusability. The adsorbent featured high Br_2 sorption capacities in both dry and humid static conditions as well as under vapor phase dynamic conditions at room temperature and elevated temperatures. Moreover, the material was found to exhibit preferential adsorption of bromine over iodine in cyclohexane. The framework showed the ability to extract aqueous phase bromine at low concentration, from 13 parts per million (ppm) down to 4 ppm, with a removal efficiency of 86.3% within less than 3 hours and high selectivity. In addition, the highly efficient continuous flow-through process for bromine extraction from water as well as the selective separation of Br_2 under dynamic conditions with great scalability and affordability have been demonstrated using COF membranes.

Results and discussion

Materials synthesis and characterization

To construct the functionalized porous adsorbents, three β-ketoenamine COFs were synthesized *via* the condensation of 4,4′,4″-(1,3,5-triazine-2,4,6-triyl)trianiline as a primary amine building block with three different aldehydes *i.e.*, 2-hydroxybenzene-1,3,5-tricarbaldehyde (1-OH), 2,4-dihydroxybenzene-1,3,5-tricarbaldehyde (2-OH), and 2,4,6-trihydroxybenzene-1,3,5-tricarbaldehyde (3-OH), to construct COF-1, COF-2 and COF-3, respectively (Fig. 1a–c and Fig. S5–S7, ESI†). By changing the aldehydes as a major building unit of these COFs, the number of hydroxyl groups (OH) was systematically tuned,

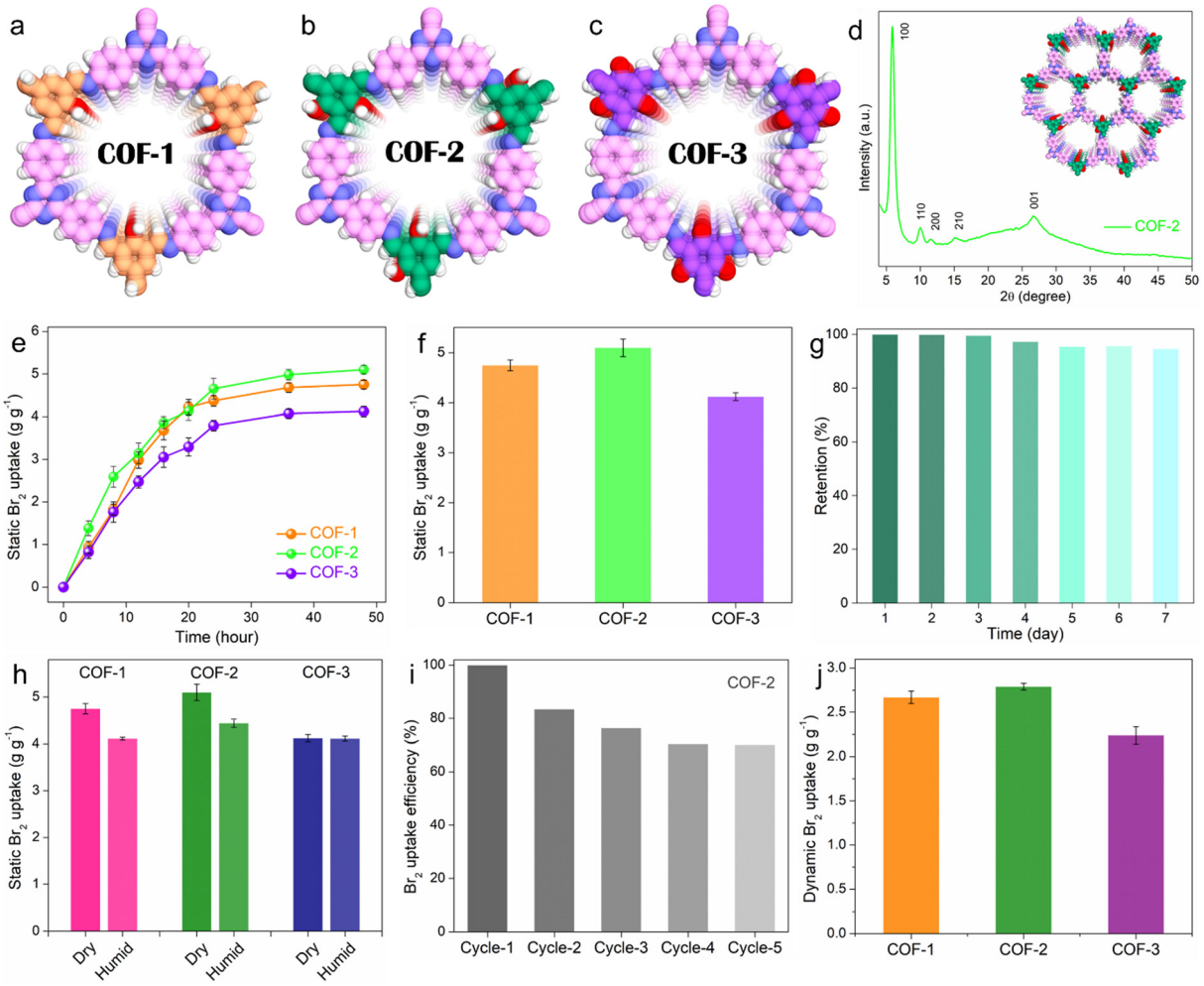

Fig. 1 Structures, characterization and results of vapor phase bromine capture test of the COFs: (a)–(c) schematic representation of the 2D structural units of COF-1, COF-2, and COF-3, respectively. (d) PXRD profile of COF-2. (e) Gravimetric measurement of static Br_2 adsorption capacities of COF-1, COF-2 and COF-3 as a function of time at 298 K. (f) Maximum static Br_2 adsorption capacities of the COFs. (g) Br_2 retention efficiency profile of COF-2. (h) Br_2 uptake capacities of the COFs under dry and humid conditions. (i) Recyclability result of COF-2 for Br_2 capture. (j) Br_2 uptake capacities of the COFs under dynamic conditions at 298 K.

which resulted in the alteration of intramolecular interactions along with conjugation, aromaticity, hydrogen bonding, and steric effect. Consequently, COFs such as enol-imine and ketoenamine can be produced.[33] For instance, herein, for COF-1 or COF-2, an enol-imine is first formed *via* the condensation reaction of the respective aldehyde and amine, followed by a reversible proton isomerization reaction to generate a more stable ketoamine form.[29] Conversely, the ketoamine form predominates in COF-3 due to the presence of three –OH groups on the trialdehyde monomers.[34] Although this encourages a very stable structure, more carbonyls with strong electron-acceptor properties can lessen their ability to interact with target analytes that are electron-deficient, such as bromine. Apart from this, these designed COFs exhibit unique characteristics, including highly crystalline chemically robust structures, large surface areas, heteroatom functionalities (triazine, imine moieties), and electronically rich frameworks, all of which are needed for selective and strong preferential binding affinity towards bromine molecules. Initially, powder X-ray diffraction (PXRD) analysis was applied in order to reveal the crystalline and phase pure nature of the as-prepared COFs. All these COFs demonstrate highly crystalline structures, and the PXRD peaks were found to match well with the reported 2D eclipsed (AA) stacking models, indicating the successful formation of these COFs (Fig. 1d and Fig. S8–S10, ESI†).[35] As an example, COF-2 exhibits the first intense peak at about 5.57°, which corresponds to the 100 reflection plane, whereas relatively weak intense peaks at 9.71°, 11.19° and 14.68° are ascribed to the 110, 200, and 210 planes, respectively. Moreover, the diffraction peak of the 001 plane at about 26.49° indicates the π–π stacking of the 2D COF. These investigations also revealed that each COF possessed a porous framework that was isostructural and featured hexagon-shaped one-dimensional pores.[36] Hereafter, the other structural and morphological analyses of all the COFs were conducted through a combination of Fourier transform infrared (FT-IR) spectroscopy, solid-state ^{13}C cross-polarization magic-angle-spinning nuclear magnetic resonance (CP-MAS NMR) spectroscopy, X-ray photoelectron spectroscopy (XPS), nitrogen gas sorption studies, field emission scanning electron microscopy (FESEM), transmission electron microscopy (TEM), and others, which have been discussed in detail in the ESI† file (Section S3 and Supporting note 1–7) and (Fig. S11–S30, ESI†).

Bromine adsorption studies

The sequestration of halogens such as bromine or iodine is important under both static and dynamic conditions. Initially, the gaseous Br_2 adsorption capacities of these COFs were evaluated under static conditions at 298 K and ambient pressure using a typical experimental setup (see ESI† file for detail, Fig. S32). As a result of this gravimetric static kinetic test, all the COFs exhibited high Br_2 adsorption capacities in the range of 4.12–5.16 g g^{-1} within 48 h of contact time (Fig. 1e). The potent combination of high porosity or surface area, abundant N-containing functional moieties such as imine and triazine, as well as phenolic hydroxyl groups within their rigid structures are responsible for the high Br_2 adsorption capabilities of these materials. Interestingly, the saturation Br_2 sorption capacities of these COFs were found to be different. Among all, COF-2 exhibited the highest maximum capacity of 5.16 g g^{-1}, whereas the capacities of COF-1 and COF-3 were 4.75 and 4.12 g g^{-1}, respectively (Fig. 1f). This difference in capacities clearly demonstrated the role of functionalities in addition to the porosities of these COFs in promoting bromine adsorption, which has been discussed in detail in the mechanism section. To the best of our knowledge, the static Br_2 uptake capacity of COF-2 is the highest value reported for any adsorbent under similar conditions (Table S1, ESI†). Adsorption kinetics is another crucial parameter for an adsorbent in addition to equilibrium adsorption capacity. The kinetics of the static Br_2 adsorption test were found to follow the pseudo second order model with very high rate constant values of 0.00703, 0.01158, and 0.00839 g g^{-1} h^{-1} for COF-1, COF-2, and COF-3, respectively (Fig. S33, ESI†). These results indicate the fast accumulation of bromine molecules within the functional pores of the COFs.

Retention efficiency is an important parameter for an ideal adsorbent and was tested by exposing the bromine-loaded COFs (Br_2@COFs) to air under ambient conditions for 1–7 days. After seven days, it was observed that Br_2@COFs retained most of their weight, suggesting that the strong interaction between the COF and Br_2 molecules is what causes the adsorption rather than surface condensation (Fig. 1g and Fig. S34, S35, ESI†). In contrast, liquid bromine was shown to evaporate entirely in less than an hour of exposure in a related investigation. These results indicate the significantly high Br_2 retention potency of these COFs. Since under practical conditions bromine gas inevitably exists with moisture, it is important to investigate the Br_2 sorption performance of the COFs in the presence of water or in humid conditions. With this aim, the Br_2 adsorption capacities of all the COFs were calculated in humid conditions at 298 K by introducing water into the Br_2 capture experimental setup. It was found that the presence of water caused a decrease in the Br_2 sorption capacities of COF-1 (from 4.75 to 4.11 g g^{-1}) and COF-2 (from 5.16 to 4.44 g g^{-1}), whereas the uptake capacity of COF-3 was found to be almost unchanged for both dry and humid conditions (Fig. 1h). This finding suggests that these adsorbents are suitable for real-world Br_2 capture applications. For an adsorbent to be fully utilized in an efficient manner in the long run, its recyclability is a crucial property. To this end, a reusability test was performed taking COF-2 as a model adsorbent. The adsorbed Br_2 in the COF can be easily extracted by treating Br_2@COF with various polar solvents such as DMSO, DMF, and THF (Fig. S36, ESI†). When treated with DMSO, the Br_2 release or desorption process proceeded spontaneously and became incremental as the contact time increased (Fig. S37 and S38, ESI†). Consequently, the recyclability test revealed that COF-2 had a high adsorption efficiency, exceeding 70% in five consecutive cycles of adsorption and desorption (Fig. 1i). The good stability and long-term use of the adsorbent towards the capture of bromine were validated by these results.

In addition to the static phase, bromine adsorption under dynamic conditions at a certain temperature and pressure provides a more precise depiction of the adsorption performance at

parameters that are close to reality. The majority of earlier research solely examined the capacity for Br_2 adsorption under static conditions, ignoring the practical importance of Br_2 adsorption in dynamic conditions. Nevertheless, the measured adsorption capacity does not accurately represent the Br_2 capture performance of the adsorbent in real-world applications since the partial pressure and, consequently, volumetric concentration of Br_2 in static conditions are much higher than the actual concentration found in practical conditions.[16] Therefore, the dynamic Br_2 adsorption capacity of these COFs was evaluated using a home-made setup with a fixed-bed column. In a typical experiment, Br_2 vapor was allowed to pass through the COF-embedded column under the flow of nitrogen as the carrier gas at 298 K (Fig. S39, ESI†). As a result of this dynamic test, COF-1, COF-2 and COF-3 exhibited saturation adsorption capacities of 2.67, 2.79 and 2.24 g g^{-1}, respectively, in dry conditions (Fig. 1j). Interestingly, the order of the capacities was found to be consistent with the static adsorption result. It should be mentioned that to the best of our knowledge, this is the first report on porous materials-based vapor phase dynamic Br_2 capture test with large adsorption capacities.

Adsorption mechanism investigation

The gaseous Br_2 adsorption results indicated that COF-2 demonstrated the highest Br_2 uptake capacities under both static and dynamic conditions compared with COF-1 and COF-3. This might be owing to the collective effect of a higher number of accessible functional sites and a large surface area of COF-2 than the others. Now, in order to gain an insight into the Br_2 adsorption mechanism and the reason behind this difference in capacities, detailed mechanistic studies were conducted using various state-of-the-art characterizations. At first, the EDX analyses using both FESEM and TEM were performed with Br_2-loaded COFs (Br_2@COFs), which exhibited the clear appearance of a large amount of bromine in the COFs structure (Fig. S40 and S41, ESI†). Also, the corresponding elemental mapping images of Br_2@COFs revealed the homogeneous distribution of bromine throughout the surface of all the COFs (Fig. S40, ESI†). A similar observation was noted for the high-resolution elemental mapping images (from TEM) of Br_2@COFs (Fig. S41, ESI†). The FESEM images of Br_2@COFs showed that the surface morphologies of the COFs remained essentially intact following Br_2 adsorption, confirming the remarkable stability of the COFs (Fig. S42, ESI†). The TEM and HRTEM images of the Br_2-loaded COFs were likewise found to be identical to those of the pristine COFs, suggesting that the materials had exceptional morphological stability after Br_2 sorption (Fig. S43, ESI†). A significant quantity of Br_2 was trapped inside the COFs' pores during adsorption, as evidenced by the TGA profiles of Br_2@COFs, which showed sustained weight loss up to almost 200 °C upon heating (Fig. S44, ESI†). These findings verified that Br_2 molecules were successfully loaded into the COFs' framework.

Thereafter, to access the potential interactions between the COFs and Br_2 molecules, FT-IR and XPS analysis were performed with the bromine-loaded COFs. The FT-IR spectra of the Br_2@COFs exhibited retention of the major peaks similar to that of pristine COFs, indicating their chemical stability towards Br_2 adsorption (Fig. S45–S47, ESI†). However, after bromine capture, the characteristic peak associated with the –C═O stretching frequency at ∼1728 cm^{-1} was found to increase notably. This finding suggests the oxidation of the phenolic hydroxyl units present in the COF structures to carbonyl groups upon interaction with bromine.[6] This observation was further investigated with the time-resolved FT-IR spectra of Br_2-loaded COF-2, which manifested significant step-wise increase in the –C═O bond frequency upon incremental contact time with bromine vapor (Fig. 2a). Nevertheless, in the case of COF-3, such oxidation of the phenolic hydroxyl groups after Br_2 capture was not so prominent. Moreover, a detailed discussion about the other potential interactions between bromine and different functional groups such as imine, triazine, and phenyl rings of the COFs is provided in supporting note 8 (ESI†). All these shifts/changes in the FT-IR spectra of Br_2@COFs indicated significant interaction between the COFs and bromine molecules through the formation of strong charge-transfer complexes.[11,16] The XPS survey spectra of Br_2@COFs exhibited the appearance of two new characteristic Br 3d signals at ∼70.28 eV and ∼71.38 eV corresponding to Br_3^- and Br_5^-, respectively (Fig. 2b and Fig. S48–S50, ESI†).[6,37] This data indicated the successful adsorption of bromine in the structure of the COFs. More importantly, for the O 1s XPS spectra of the COFs, it was discovered that following bromine adsorption, the intensity of the peak at ∼531.8 eV due to the –C═O group was increased, whereas the corresponding signal of O 1s from the –C–OH unit at ∼533.5 eV decreased (Fig. 2c and Fig. S51, ESI†). These results, in addition to the FT-IR results, also confirmed that upon Br_2 adsorption, the phenolic hydroxyl groups were oxidized to –C═O groups.[6] Additionally, the signals associated with the N 1s and C 1s XPS spectra of the COFs after bromine adsorption were found to be shifted slightly compared to those of pristine COFs, suggesting the involvement of these atoms or their corresponding moieties towards the interaction with bromine molecules (Fig. S52 and S53, ESI†). These findings unequivocally showed that charge-transfer complexes were formed by the trapped bromine molecules interacting with the functional groups of the COF structures, specifically at the redox-active phenolic hydroxyl groups, imine-N, triazine-N, and electron-rich phenyl sites.[5,6,13,16]

Furthermore, Raman spectroscopy was applied to identify the bromine species adsorbed within the porous COF structures. The bromine-loaded COFs demonstrated Raman bands located in the range from ∼173 cm^{-1} to 325 cm^{-1}, which were not present for the pristine COFs (Fig. S54, ESI†). These bands are majorly associated with the symmetric and/or asymmetric stretching vibration of the polybromide species such as Br_3^- and Br_5^- as well as the Br_2 molecule (Fig. 2d).[13,38–40] These results revealed that bromine molecules were identifiable in the COFs as pure molecules as well as polybromide species (Br_3^- and Br_5^-). Furthermore, using a mapping study of Raman spectroscopy, the spatial distribution of bromine species within the COF-2 structure was examined (Fig. S55, ESI†).

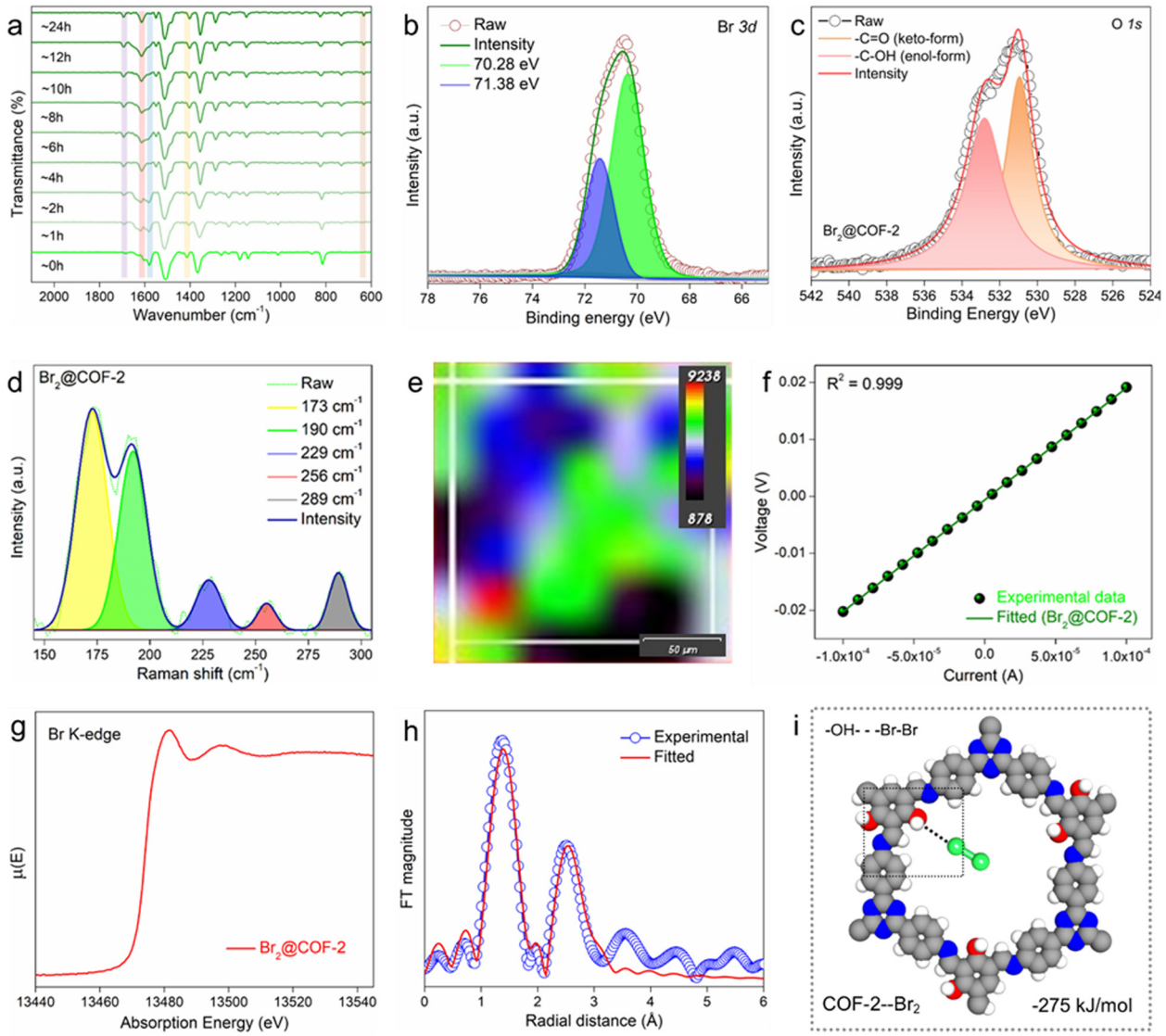

Fig. 2 Results of bromine adsorption mechanism studies: (a) time-dependent FT-IR spectra of Br_2@COF-2. (b) and (c) Br 3d and O 1s XPS spectra of Br_2@COF-2, respectively. (d) and (e) Raman spectra and corresponding colour mapping of Br_2@COF-2. (f) Current *vs.* voltage spectra of Br_2@COF-2. (g) and (h) Bromine K-edge XANES spectra and corresponding FT magnitude of Br_2@COF-2. (i) DFT energy-optimized structures and corresponding binding energy of bromine interacting with the –OH functionalities of COF-2.

The distribution of adsorbed bromine species with substantial intensities of different bands is displayed in the colour-coded Raman mapping of Br_2@COF-2 (Fig. 2e). The image indicated the peak position maps of the Raman signals of the loaded bromine molecules or species within the COF-2 structure. Moreover, the formation of charge-transfer complexes between the adsorbed bromine species and the COFs structure was evidenced by the solid-state UV-vis spectra of the Br_2@COFs, which exhibited characteristic broad absorption signals (Fig. S56, ESI†).[41] Additionally, there is a noticeable broadening of the signals in the solid-state ^{13}C CP-MAS spectra of Br_2@COFs after Br_2 capture (Fig. S57, ESI†). The reason for this could be the strong interaction between the electron-deficient bromine molecules and the π-electron rich COF moieties.[17,42,43] The electrical conductivities (σ) of the bromine-loaded COFs were evaluated, which exhibited bulk σ values of approximately 2.58×10^{-3}, 2.71×10^{-2}, and 5.05×10^{-3} S cm^{-1} for COF-1, COF-2 and COF-3, respectively (Fig. 2f and Fig. S58, ESI†). These calculated values indicated that excess bromine or polybromide anions had been successfully occupied in the pores of COFs.[37,43] Additionally, we recorded the extended X-ray adsorption fine structure (EXAFS) data of the bromine-loaded COF-2 sample, which indicated the appearance of distinct peaks associated with the Br K-edge (Fig. 2g, h and Fig. S59, Table S2, ESI†). This analysis further supported the successful grafting of bromine within the COF-2 structure. Finally, the lack of diffraction peaks in the PXRD patterns of Br_2@COFs suggested that amorphous bromine had been loaded into the COFs' pores (Fig. S60, ESI†). All of these results showed that the simultaneous action of physisorption and chemisorption contributed to the selective

adsorption of the bromine species by means of various multiple functionalities, such as phenolic hydroxyl groups, phenyl moieties, and heteroatomic sites such as triazine and imine of the COFs.

We were also urged to provide an understanding of the process underlying the three COFs' differing capabilities for adsorbing Br_2 (order of capacity as COF-2 > COF-1 > COF-3) using their structure-properties correlations. It was demonstrated in the above discussion that the phenolic hydroxyl groups of COFs serve as one of the vital interaction sites for the selective adsorption of bromine through oxidation to –C═O groups.[6] Now, it is established in the literature that under dry conditions, the structures of COF-1 and COF-2 exhibited both enol and keto configurations (Fig. S61, ESI†).[27,44] Nevertheless, only the keto form of these COFs exist in humid conditions. Conversely, in the case of COF-3, keto–enol tautomerism results in the keto form being dominant in both dry and humid conditions (Fig. S61, ESI†).[27,35] All these indicate that in dry conditions, COF-2 exhibits a higher concentration of phenolic hydroxyl groups (enol form) when compared to the other two COFs, resulting in COF-2 having a larger adsorption capacity for Br_2 than COF-1 and COF-3. However, a notable decrease in the Br_2 adsorption capacity was seen under the humid conditions as the quantity of the phenolic hydroxyl groups of COF-2 decreased (Fig. 1h). A comparable observation was also made on COF-1. It is noteworthy that in the case of COF-3, there was no discernible impact of humidity on the capacity to adsorb Br_2; this is presumably due to the absence of phenolic hydroxyl sites in both dry and humid conditions (Fig. 1h). In addition to this, the relatively higher porosity of COF-2 than the other two COFs also led to the highest Br_2 adsorption capacity.[45]

Further, to gain more insights into the preferred adsorption configurations of Br_2 at different functional sites such as phenolic hydroxyl groups, triazine, and imine sites of the COFs, density functional theory (DFT) calculations were employed (Section S7, ESI†). All these sites have potential for interaction with the Br_2 molecule. To evaluate these interactions, the energy-optimized structures and their corresponding binding energies were calculated using the Becke, 3-parameter, Lee–Yang–Parr (B3LYP) exchange–correlation function, considering the repeating units of the COFs as model molecules to represent their structures. The calculation showed that COF-1 and COF-2 interact with Br_2 molecules *via* –OH groups with binding energies of -258 and -275 kJ mol^{-1}, respectively (Fig. 2i and Fig. S63–S65, ESI†). The binding energies for other interactions of all the COFs are shown in Fig. S63–S65 (ESI†). The overall theoretical results supported the aforementioned experimental findings by showing that in addition to other factors, the phenolic hydroxyl groups of the COFs are the most preferred binding site for Br_2 adsorption.[46–49]

Solution-phase bromine separation studies

The above mechanistic studies established COF-2 as the most potential adsorbent among others owing to its higher number of accessible functional binding sites and large porosity. Therefore, the following solution-phase Br_2 capture studies were performed with COF-2 as a model adsorbent. At first, during the kinetic experiment in cyclohexane, COF-2 was found to decrease the concentration of Br_2 quickly as the UV-vis intensity of Br_2 in cyclohexane decreased sharply with time (Fig. 3a and b). The brown colour of the solution steadily diminished over the period of three hours, finally becoming colourless, as observed by naked eye (Fig. S66, ESI†). The kinetic data indicated that almost ~80% removal efficiency was achieved within 5 min of contact time, whereas it was ~96% within 3 hours from an initial feed solution of 4 mM Br_2 in cyclohexane (Fig. 3b). The result was found to follow the pseudo-second-order kinetic model with a high rate constant value of k_{obs} = 0.14879 g mg^{-1} min^{-1} (Fig. S67, ESI†). Furthermore, the Br_2 adsorption capacity in cyclohexane was evaluated at room temperature taking a 20 mM stock solution. From the UV-vis spectra, it was found that the saturation capacity of COF-2 was reached within 360 min, and the maximum Br_2 capacity was calculated to be 3.92 g g^{-1} (Fig. S68, ESI†). To the best of our knowledge, the Br_2 saturation capacity of COF-2 in cyclohexane was one of the highest among those of the reported materials (Table S3, ESI†).

Inspired further by a recent study by Chi and Sessler *et al.*[6] that showed effective bromine isolation from a mixture of I_2 and Br_2 using calix[4]pyrrole-based POP, we aimed to investigate the efficacy of our material in the preferential separation of Br_2 from a halogen mixture. Research on the selective separation of particular halogens (bromine) from others (iodine) is highly regarded because it is crucial to many different sectors. Nevertheless, the fact that I_2 and Br_2 coexist in equilibrium with inter-halogen molecules like IBr makes the extraction of bromine from iodine difficult.[50,51] Therefore, before the selective bromine extraction study in cyclohexane, we performed the individual bromine and iodine capture kinetic study with COF-2. According to the UV-vis result, within 3 hours of contact, COF-2 was found to decrease ~97% Br_2 concentration from 4 mM stock solution, whereas only ~15% decrement in I_2 concentration was noted even in the case of 2 mM stock I_2 solution (Fig. 3b, c and Fig. S69, ESI†). This result motivated us further to investigate the selective separation of bromine from the mixture of Br_2, I_2 and IBr.[6] As a result of this test, the UV-vis spectra indicated that the absorption maximum of the mixture of Br_2, I_2, and IBr gradually redshifted over time, resulting in a final spectrum that matched the spectrum of I_2 in cyclohexane (Fig. 3d).[6] The preferential interaction of bromine with COF-2 over iodine in cyclohexane is likely what caused this phenomenon, shifting the equilibrium away from IBr and toward free Br_2 and I_2. This phenomenon was observed by the naked eye as well (Fig. 3e and Fig. S70, ESI†). All of these findings suggested that COF-2 might be used as an adsorbent to separate bromine from other impurities such as I_2 and IBr.

As indicated previously, because of its high reactivity and potential effects on the environment and human health, bromine must be removed from the aqueous phase. Bromine is frequently found in wastewater streams from a variety of industrial activities, such as the production of chemicals, electronics, and wastewater treatment facilities. If released into the environment, bromine can contribute to the formation of

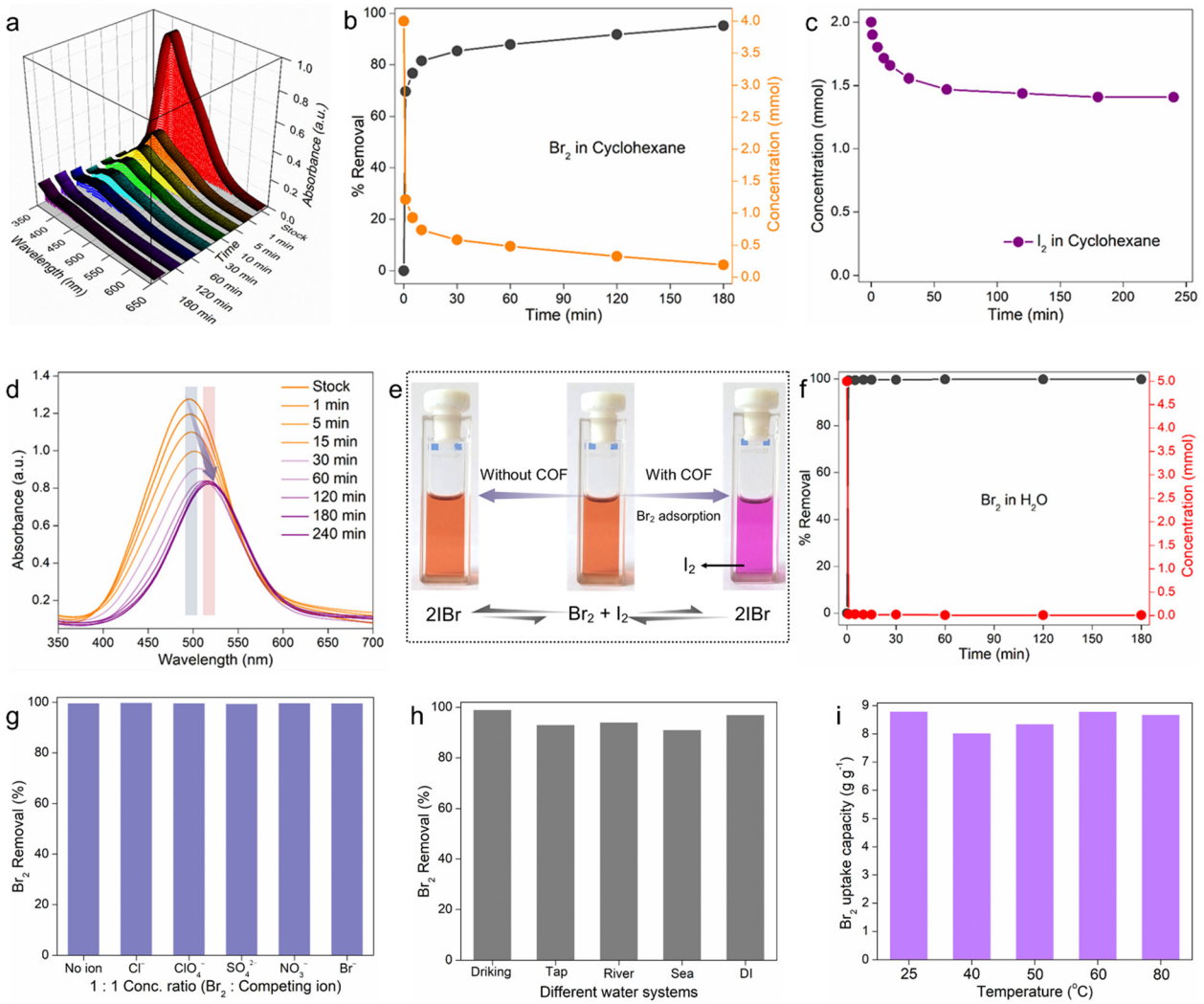

Fig. 3 Solution-phase bromine separation results: (a) UV-vis spectra of the Br_2 capture test in cyclohexane. (b) %removal efficiency and concentration decrease of Br_2 in cyclohexane as a function of time. (c) Concentration decrease of iodine with time in cyclohexane. (d) The change in the UV/vis absorption spectrum with time of an initial bromine and iodine mixed cyclohexane solution. (e) Images of colour changes observed during the selective Br_2 adsorption test in cyclohexane. (f) %removal efficiency and concentration decrease of Br_2 in water as a function of time. (g) Selectivity result for Br_2 capture in water. (h) Result of Br_2 capture in different water systems. (i) Br_2 capture capacities of COF-2 at different temperatures.

harmful byproducts, such as brominated disinfection byproducts (DBPs), which are known to be more toxic than their chlorinated counterparts.[52] The National Sanitation Foundation (NSF) recommends a total bromine/bromide intake level of 10 ppm for drinking water due to its extreme toxicity.[9] Thus, removing bromine from the aqueous phase lessens the possibility of environmental contamination and hazards to human health and ecosystems. It should be noted that most of the bromine uptake experiments that have been reported have focused primarily on the exchange capacity and have only shown vapor-phase bromine capture.[52] However, there has been limited focus on the selective extraction of bromine from its high concentration aqueous solutions in the presence of an excess of other interfering anions, even though it is essential for real-time water treatment applications. Moreover, no studies have focused on the adsorption of bromine from its very low concentration aqueous solutions. Therefore, COF-2 was used to assess bromine's capacity to be adsorbed from both high and low concentration aqueous solutions. Initially, at high concentration, the Br_2 removal kinetic study revealed a sharp decrease in the UV-vis intensities as well as corresponding visual colours changes with increasing time, suggested the removal of Br_2 from water (Fig. S71 and S72, ESI†). The feed concentration (5 mM) was found to decrease quickly as almost 99% Br_2 removal efficiency was observed within 1 min of treatment time (Fig. 3f). The Br_2 adsorption kinetics in water fitted well with the pseudo-second-order model with a high rate constant value of 10.21 g mg^{-1} min^{-1}, further suggesting chemisorption as the active mechanism of Br_2 sorption (Fig. S73, ESI†).[53] Thereafter, the saturated Br_2 uptake capacity of COF-2 in water was evaluated taking 30 mM stock aqueous solution. The time-dependent capacity test revealed 8.79 g g^{-1} Br_2 adsorption capacity of COF-2 in water (Fig. S74, ESI†), which was found to be one of the highest when compared with the reported materials.[15]

In addition to the high concentration aqueous phase Br_2 uptake studies, the adsorption of trace Br_2 with very low concentration from water was also investigated. The inductively-coupled plasma mass spectroscopy (ICP-MS) analysis result indicated that COF-2 was able to reduce the initial trace Br_2 concentration ($\sim$13 ppm) to below $\sim$4 ppm within 1 hour as more than 70% Br_2 was removed within that time frame (Fig. S75, ESI†). Next, inspired by such fast and efficient sequestration of molecular bromine from water by COF-2, a series of other important Br_2 adsorption tests was further examined. In practical conditions, the presence of additional coexisting anions such as SO_4^{2-}, NO_3^-, ClO_4^-, Br^-, and Cl^- in Br_2-contaminated water can have an adverse influence on the sorption efficacy of the adsorbent. Therefore, the selectivity test of Br_2 (in high concentration) capture in the presence of the above competing anions was performed. Notably, COF-2 demonstrated the highly efficient separation of Br_2 with a removal efficiency of $>$ 97% in case of all the anions, further exhibiting high selectivity towards Br_2 molecule (Fig. 3g). Furthermore, after evaluation, the corresponding K_d values for each anion were calculated to be in the range of $\sim 10^5$ mL g^{-1}, indicating that COF-2 has an exceptionally high binding affinity for Br_2 (Fig. S76, ESI†). Encouraged by this effective and selective trapping of Br_2 by COF-2 in water, additional Br_2 sequestration from various complex water matrixes, such as drinking water, tap water, seawater, DI water, and river water, was carried out. Remarkably, the adsorbent demonstrated about 89% bromine removal effectiveness in just five minutes across all water systems (Fig. 3h).

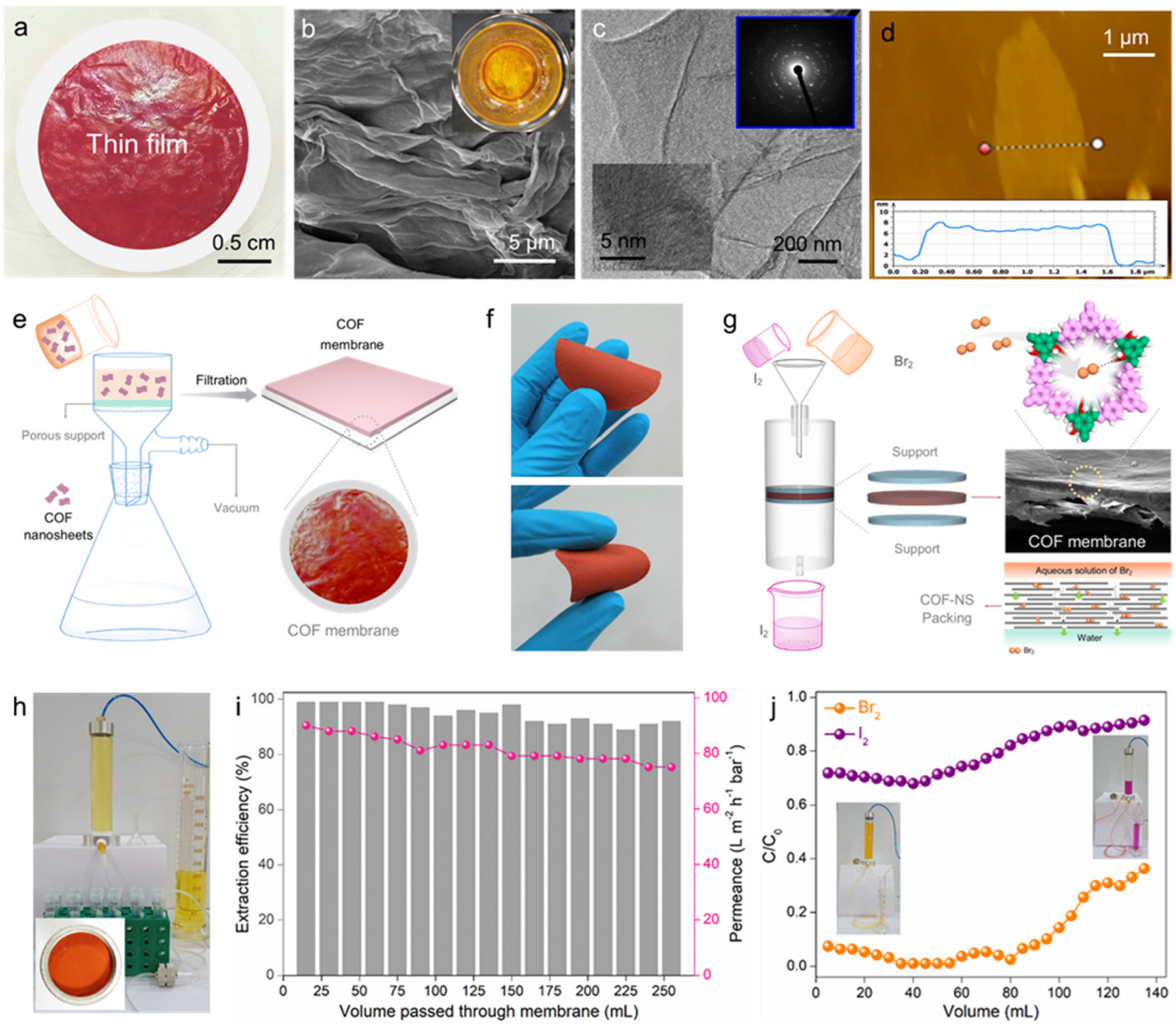

Fig. 4 Characterization of the COF-2 membrane and the result of continuous flow-through Br_2 and I_2 separation tests: (a) Digital image of COF-2-TF. (b) Cross-sectional FESEM images of COF-2-TF. (c) TEM images of COF-2-TF (inset: HRTEM and SAED image). (d) AFM image and the corresponding height profile of COF-2-TF. (e) Schematic illustration for the fabrication of the COF-2 membrane *via* the vacuum filtration method. (f) Digital images of the COF-2 membrane. (g) Schematic representation of the dynamic column-based flow-through technique for bromine and iodine capture using the COF-2 membrane. (h) Image of the COF-2 membrane installed in a separation chamber. (i) Result of the Br_2 extraction efficiency and permeance for a large volume of Br_2-contaminated water. (j) Result of the dynamic Br_2 and I_2 capture test in cyclohexane using the COF-2 membrane.

Lastly but importantly, a crucial test was conducted using the aqueous phase for Br_2 sorption at increased temperatures. The results showed that the adsorbent had good saturation capacities for bromine at all temperatures (Fig. 3i).

Membrane-based continuous bromine separation studies

Furthermore, to demonstrate the potential of COF-2 in scalable bromine adsorption, we also developed a scheme involving a continuous flow-through-based Br_2 capture through COF-2 membranes. The separation of the targeted chemicals over two dimensional-based films/membranes (such as COF membranes) *via* adsorption constitutes an appealing strategy, featuring simple and large-scale purification application. In comparison to traditional powder counterparts, 2D-COF-based membranes have several added advantages as efficient adsorbents. Among them, the well-organized formation of COF thin nanosheets into membranes enhances their environmental stability and hence increases their lifetime for superior and repeatable separation performance. Furthermore, following separation application, recycling the COF-based membrane is simpler, faster, and less expensive than recycling its powder counterpart. Recently, owing to the multifunctional properties of 2D COFs, there has been high topical research interest in the field of high-quality membrane preparation and their utility in various leading applications.[30,54–57] To test dynamic Br_2 adsorption, a large area-based robust thin-film of COF-2 was first constructed *via* a single-step dual organic-phase interfacial crystallization method following a protocol described in the ESI† file (see details in Section S9). The as-synthesized COF-2 film (COF-2-TF) was found to be free-standing with about 6 cm diameter and dark red colour (Fig. 4a and Fig. S77, ESI†). Interestingly, the COF-2-TF could be easily exfoliated into nanosheets *via* ultrasound treatment. The cross-section FESEM images of COF-2-TF exhibited an assembly of a large number of nanosheets stacked one over another (Fig. 4b and Fig. S78, ESI†). Also, the top view FESEM images showed a relatively smooth surface of the COF-2-TF. The TEM image of COF-2-TF displayed ultrathin layers/nanosheets-like morphology, whereas the HRTEM and SAED images indicated the well-ordered stacking of clear lattice fringes and diffraction spots of the crystalline COF layers (Fig. 4c and Fig. S79, ESI†).[56,57] Moreover, atomic force microscopy (AFM) analysis of the COF-2-TF was performed, which revealed the layer or sheet-like structure of the material with an average thickness of about 8 nm (Fig. 4d and Fig. S80, ESI†). The crystalline structure of the nanosheets of COF-2-TF was evaluated by PXRD, which explored a similar pattern to its powder counterpart (Fig. S81, ESI†). The ^{13}C CP-MAS solid-state NMR spectra of COF-2-TF indicated the presence of all the relevant functional groups within the structure, which support the formation of the COF backbone (Fig. S82, ESI†). Additionally, the FTIR spectra and other relevant characterization results validate the structure of COF-2-TF (Fig. S83 and S84, ESI†). Finally, the porous structure of COF-2-TF was examined by low-temperature N_2 gas sorption analysis (Fig. S85, ESI†).

Thereafter, the COF-2 membrane was fabricated over a porous support applying vacuum-assisted filtration method using an aqueous suspension of COF-2 nanosheets (Fig. 4e) (see Section S10 for detailed preparation, ESI†). Thus, the developed COF-2 membrane was found to have a well-defined structure with robust mechanical strength due to the strong π–π interaction between the interlayers of the tiny nanosheets (Fig. 4f). The top-view and cross-sectional FESEM image of the membrane display the uniform packing of nanosheets with a smooth surface morphology and average membrane thickness of 50 μm, respectively (Fig. S86, ESI†). Notably, the packing of COF nanosheets in the membrane manifested a graphene oxide membrane with a laminar structure, which is beneficial for the molecular separation study (Fig. 4g).[58,59] Moreover, the accessible functional groups on COF nanosheets/membrane also intensified the interactions with specific analytes.

The fast, efficient and selective adsorption of molecular bromine from water by COF-2 led us to consider that the COF-2 membrane might allow bromine capture under dynamic flow-through conditions, which is more important for practical application. Aqueous phase dynamic Br_2 sequestration was carried out using a homemade setup in order to evaluate this potential (Fig. 4h and Fig. S87, ESI†). Initially, a column installed with COF-2 membrane was used to filter a 5 mM stock solution of Br_2 in water. The eluent was then examined using UV-vis spectroscopy. It was found that even after passing more than 200 mL of Br_2-contaminated water, the COF-2 membrane was able to remove bromine with an efficiency of $> 90\%$ (Fig. 4i). Also, the permeance of the COF-membrane was calculated to be above 60 L m^{-2} h^{-1} bar^{-1} throughout the whole Br_2 separation process. This finding investigates the potential use of the COF-2 membrane in large-scale, practical flow-through bromine capture from water. Moreover, the effective bromine adsorption but ineffective iodine uptake of COF-2 further inspired us to investigate the performance of the COF-2 membrane towards the comparative elimination of Br_2 and I_2 from a cyclohexane solution under dynamic conditions (Fig. 4g). In this typical experiment, separate 2.5 mM stock solutions of Br_2 and I_2 in cyclohexane were run through the column, and UV-vis spectroscopy was used to determine the eluent concentrations. The COF-2 membrane demonstrated over 90% effectiveness in removing Br_2 through a continuous flow-through adsorption test. This performance was maintained when passing about 80 millilitres of Br_2 cyclohexane solution in the dynamic mode (Fig. 4j and Fig. S88, ESI†). On the flip side, in case of the I_2 adsorption test, the COF-2 membrane manifested inadequate removal efficiency as very less sequestration of I_2 was observed during the whole dynamic process (Fig. 4j and Fig. S89, ESI†). Drawing from the outcomes of the dynamic experiment involving the capture of Br_2 and I_2, we believe that the COF-2 membrane may play a potential role in the selective separation of Br_2 from other halogens, such as I_2, in a flow-through mechanism.

Conclusions

To summarize, this study showcased a methodical examination of extremely effective bromine gas sequestration from the vapor

phase by the development of three chemically stable functionalized COFs. Out of all the materials that have been reported to date, COF-2 functionalized with a redox-active phenolic di-hydroxyl group and high porosity was found to exhibit a record-breaking Br_2 adsorption capacity in both static and dynamic conditions, with large retention efficiency and admirable recyclability. Under static conditions, COF-2 was found to efficiently adsorb gaseous bromine with a high adsorption capacity of 5.16 g g^{-1}, whereas under dynamic conditions, the saturation capacity was 2.79 g g^{-1}. Moreover, COF-2 was capable of eliminating molecular bromine from cyclohexane solution with fast sorption kinetics and high uptake capacity (3.92 g g^{-1}). The selective adsorption of bromine in the presence of potential interferents, such as iodine, was also demonstrated by COF-2. COF-2 was found to efficiently and selectively remove a large amount of Br_2 from water in the presence of other competing anions. Furthermore, COF-2 could eliminate trace bromine in aqueous medium from concentrations of 13 ppm down to as low as 4 ppm. More significantly, in an individual dynamic flow-through capture test, the COF-2 membrane demonstrated highly effective continuous Br_2 adsorption from water as well as the preferable continuing sequestration of Br_2 in cyclohexane over I_2. This work highlights how crucial it is to strike a balance between textural characteristics and strong host–guest interactions when creating adsorbents that are rationally designed to sequester bromine with high efficiency. We believe that the long-standing challenge of capturing, storing, purifying, and transporting toxic and volatile halogens such as bromine and other reactive substrates could be potentially minimized by the current approach of identifying efficient adsorbents, such as the COFs presented here.

Author contributions

S. F designed the material and performed the synthesis and characterizations. S. F., D. G., K. B., and W. M. carried out the initial sorption experiments and analysed the data. K. B. help in the preparation of the references of the manuscript. G. K. D. perform the XPS plotting and analysis. N. S., A. R., and D. M. performed few control reactions, and recorded FT-IR, PXRD and few other data. A. R. prepare the graphical structures of the COFs. R. R. U. performed the X-ray absorption (EXAFS) studies. M. M. S performed the theoretical studies. S. F. wrote the paper, while all the authors revised the manuscript. All authors discussed the results and commented on the manuscript. S. K. G. supervised the study.

Data availability

All data used for this study are available in the paper and ESI† files.

Conflicts of interest

There are no conflicts to declare.

Acknowledgements

S. F., acknowledges DST-Inspire, D. G., K. B, N. S., A. R., and A. R., acknowledges UGC, and G. K. D. acknowledges CSIR for research fellowships. W. M. and D. M. acknowledges IISER-Pune for research fellowships, respectively. We wish to acknowledge Dr Biplab Ghosh, Scientific Officer (G), and Scanning EXAFS Beamline (BL-9), Indus-2, Beamline Development & Application Section (BDAS), BARC, Mumbai for EXAFS facilities. S.K.G thanks DST-SERB project (CRG/2022/001090) and MoE-STARS/STARS-2/2023-0218 for funding.

Notes and references

1 R. B. McDonald and W. R. Merriman, Special Publication, *Chem. Soc.*, 1977, **31**, 168.
2 B. Grinbaum and M. B. F. Kirk-Othmer, *Encyclopedia of chemical technology*, John Wiley, New York, 2004, vol. 4, p. 1.
3 G. L. Soloveichik, *Nature*, 2014, **505**, 163–165.
4 C. Wang, Q. Lai, K. Feng, P. Xu, X. Li and H. Zhang, *Nano Energy*, 2018, **44**, 240–247.
5 Y. Tulchinsky, C. H. Hendon, K. A. Lomachenko, E. Borfecchia, B. C. Melot, M. R. Hudson, J. D. Tarver, M. D. Korzyński, A. W. Stubbs, J. J. Kagan, C. Lamberti, C. M. Brown and M. Dincă, *J. Am. Chem. Soc.*, 2017, **139**, 5992–5997.
6 D. Chen, D. Luo, Y. He, J. Tian, Y. Yu, H. Wang, J. L. Sessler and X. Chi, *J. Am. Chem. Soc.*, 2022, **144**, 16755–16760.
7 K. Watson, M. J. Farré and N. Knight, *J. Environ. Manage.*, 2012, **110**, 276–298.
8 F. L. Theiss, S. J. Couperthwaite, G. A. Ayoko and R. L. Frost, *J. Colloid Interface Sci.*, 2014, **417**, 356–368.
9 R. Bevan, A. Nocker and M. Sobsey, WHO Press, World Health Organization: Geneva, Switzerland, 2018.
10 J. Pang, S. Yuan, D. Du, C. Lollar, L. Zhang, M. Wu, D. Yuan, H.-C. Zhou and M. Hong, *Angew. Chem., Int. Ed.*, 2017, **56**, 14622–14626.
11 A. De, S. Haldar, J. Schmidt, S. Amirjalayer, F. Reichmayr, N. Lopatik, L. Shupletsov, E. Brunner, I. M. Weidinger and A. Schneemann, *Angew. Chem., Int. Ed.*, 2024, **63**, e202403658.
12 A. Hassan, S. A. Wahed, S. Goswami, S. Mondal and N. Das, *ACS Appl. Nano Mater.*, 2024, **7**(14), 16413–16421.
13 S. Lee, I. Kevlishvili, H. J. Kulik, H.-T. Kim, Y. G. Chung and D.-Y. Koh, *J. Mater. Chem. A*, 2022, **10**, 24802–24812.
14 Y.-P. Li, B. Xia, S. Hu, Y. Zhong, Y.-E. Huang, Z.-Z. Zhang, N. Wu, Y.-W. Wu, X.-H. Wu, X. Y. Huang, Z. Xiao and K.-Z. Du, *Energy Environ. Mater.*, 2020, **3**, 535–540.
15 C. Wang, K. Yang, Q. Xie, J. Pan, Z. Jiang, H. Yang, Y. Zhang, Y. Wu and J. Han, *Nano Lett.*, 2023, **23**(6), 2239–2246.
16 Y. Xie, T. Pan, Q. Lei, C. Chen, X. Dong, Y. Yuan, J. Shen, Y. Cai, C. Zhou, I. Pinnau and Y. Han, *Angew. Chem., Int. Ed.*, 2021, **60**, 22432–22440.
17 L. He, L. Chen, X. Dong, S. Zhang, M. Zhang, X. Dai, X. Liu, P. Lin, K. Li, C. Chen, T. Pan, F. Ma, J. Chen, M. Yuan, Y. Zhang, L. Chen, R. Zhou, Y. Han, Z. Chai and S. Wang, *Chem*, 2021, **7**, 699–714.

18 S. Salai Cheettu Ammal, S. P. Ananthavel, P. Venuvanalingam and M. S. Hegde, *J. Phys. Chem. A*, 1997, **101**, 1155–1159.
19 M. M. Naseer, A. Bauza, H. Alnasr, K. Jurkschat and A. Frontera, *CrystEngComm*, 2018, **20**, 3251–3257.
20 C. S. Diercks and O. M. Yaghi, *Science*, 2017, **355**, eaal1585.
21 S. Y. Ding and W. Wang, *Chem. Soc. Rev.*, 2013, **42**, 548–568.
22 N. Huang, P. Wang and D. Jiang, *Nat. Rev. Mater.*, 2016, **1**, 16068.
23 S. Lin, C. S. Diercks, Y. B. Zhang, N. Kornienko, E. V. Nicholes, Y. Zhano, A. R. Paris, D. Kim, P. Yang, O. M. Yaghi and C. J. Chang, *Science*, 2015, **349**, 1208–1213.
24 J. L. Segura, M. J. Manchenoa and F. Zamora, *Chem. Soc. Rev.*, 2016, **45**, 5635–5671.
25 X. Chen, K. Geng, R. Liu, K. T. Tan, Y. Gong, Z. Li, S. Tao, Q. Jiang and D. Jiang, *Angew. Chem., Int. Ed.*, 2020, **59**, 5050–5091.
26 C. R. DeBlase, K. E. Silberstein, T. T. Truong, H. D. Abruña and W. R. Dichtel, *J. Am. Chem. Soc.*, 2013, **135**(45), 16821–16824.
27 S. Kandambeth, K. Dey and R. Banerjee, *J. Am. Chem. Soc.*, 2019, **141**, 1807–1822.
28 S. Karak, K. Dey and R. Banerjee, *Adv. Mater.*, 2022, **34**, 2202751.
29 F. Chu, G. Hai, D. Zhao, S. Liu, Y. Hu, G. Zhao, B. Peng, G. Wang and X. Huang, *ACS Catal.*, 2023, **13**(20), 13167–13180.
30 S. Yuan, X. Li, J. Zhu, G. Zhang, P. V. Puyvelde and B. V. D. Bruggen, *Chem. Soc. Rev.*, 2019, **48**, 2665–2681.
31 D. W. Burke, Z. Jiang, A. G. Livingston and W. R. Dichtel, *Adv. Mater.*, 2024, **36**, 2300525.
32 J. L. Fenton, D. W. Burke, D. Qian, M. Olvera de la Cruz and W. R. Dichtel, *J. Am. Chem. Soc.*, 2021, **143**, 1466.
33 L. Zhang, S. L. Wang, G. H. Zhang, N. Shen, H. Chen, G. Tao, G. H. Tao, F. Yong, J. Fu, Q. H. Zhu and L. He, *Cell Rep. Phys. Sci.*, 2022, **3**, 101114.
34 S. Kandambeth, A. Mallick, B. Lukose, M. V. Mane, T. Heine and R. Banerjee, *J. Am. Chem. Soc.*, 2012, **134**(48), 19524–19527.
35 Y. Chen, X. Luo, J. Zhang, L. Hu, T. Xu, W. Li, L. Chen, M. Shen, S.-B. Ren, D.-M. Han, G.-H. Ning and D. Li, *J. Mater. Chem. A*, 2022, **10**, 24620–24627.
36 S. Ruidas, A. Das, S. Kumar, S. Dalapati, U. Manna and A. Bhaumik, *Angew. Chem., Int. Ed.*, 2022, **61**, e202210507.
37 W. Wu, S. Xu, Z. Lin, L. Lin, R. He and X. Sun, *Energy Storage Mater.*, 2022, **49**, 11–18.
38 A. L. Aguiar, E. B. Barros, V. P. Sousa Filho, H. Terrones, V. Meunier, D. Machon, Y. A. Kim, H. Muramatsu, M. Endo, F. Baudelet, A. San-Miguel and A. G. Souza Filho, *J. Phys. Chem. C*, 2017, **121**, 10609–10619.
39 J. C. Evans and G. Y. S. Lo, *Inorg. Chem.*, 1967, **6**, 1483–1486.
40 G. M. do Nascimento, T. Hou, Y. A. Kim, H. Muramatsu, T. Hayashi, M. Endo, N. Akuzawa and M. S. Dresselhaus, *Nano Lett.*, 2008, **8**, 4168–4172.
41 M. Leloire, C. Walshe, P. Devaux, R. Giovine, S. Duval, T. Bousquet, S. Chibani, J. F. Paul, A. Moissette, H. Vezin, P. Nerisson, L. Cantrel, C. Volkringer and T. Loiseau, *Chem. Eur. J.*, 2022, **28**, e2021044.
42 S. Fajal, W. Mandal, A. Torris, D. Majumder, S. Let, A. Sen, F. Kanheerampockil, M. M. Shirolkar and S. K. Ghosh, *Nat. Commun.*, 2024, **15**, 1278.
43 Z. Yin, Q. X. Wang and M. H. Zeng, *J. Am. Chem. Soc.*, 2012, **134**(10), 4857–4863.
44 G. H. Ning, Z. Chen, Q. Gao, W. Tang, Z. Chen, C. Liu, B. Tian, X. Li and K. P. Loh, *J. Am. Chem. Soc.*, 2017, **139**, 8897–8904.
45 S. Fajal, D. Majumder, W. Mandal, S. Let, G. K. Dam, M. M. Shirolkar and S. K. Ghosh, *J. Mater. Chem. A*, 2023, **11**, 26580–26591.
46 K. Kim and K. D. Jordan, Comparison of Density Functional and MP2 Calculations on the Water Monomer and Dimer, *J. Phys. Chem.*, 1994, **98**, 10089–10094.
47 P. J. Stephens, F. J. Devlin, C. F. Chabalowski and M. J. Frisch, Ab Initio Calculation of Vibrational Absorption and Circular Dichroism Spectra Using Density Functional ForceFields, *J. Phys. Chem.*, 1994, **98**, 11623–11627.
48 C. J. Cramer, *Essentials of Computational Chemistry: Theories and Models*, Wiley, 2nd edn, 2004.
49 S. Fajal, A. Hassan, W. Mandal, M. M. Shirolkar, S. Let, N. Das and S. K. Ghosh, *Angew. Chem., Int. Ed.*, 2023, **62**, e02214095.
50 D. S. Macnair, *J. Chem. Soc., Dalton Trans.*, 1893, **63**, 1051–1054.
51 D. Solis-Ibarra, I. C. Smith and H. I. Karunadasa, *Chem. Sci.*, 2015, **6**, 4054–4059.
52 B. Winid, *Appl. Geochem.*, 2015, **63**, 413–435.
53 Y. S. Ho and G. McKay, *Process Biochem.*, 1999, **34**, 451–465.
54 C. Zhang, B. H. Wu, M. Q. Ma, Z. Wang and Z. K. Xu, *Chem. Soc. Rev.*, 2019, **48**, 3811–3841.
55 H. Wang, Z. T. Zeng, P. Xu, L. S. Li, G. G. Zeng, R. Xiao, Z. Y. Tang, D. L. Huang, L. Tang, C. Lai, D. N. Jiang, Y. Liu, H. Yi, L. Qi, S. J. Ye, X. Y. Ren and W. W. Tang, *Chem. Soc. Rev.*, 2019, **48**, 488–516.
56 Y. Li, Q. Wu, X. Guo, M. Zhang, B. Chen, G. Wei, X. Li, X. Li, S. Li and L. Ma, *Nat. Commun.*, 2020, **11**, 599.
57 H. Wang, Y. Zhai, Y. Li, Y. Cao, B. Shi, R. Li, Z. Zhu, H. Jiang, Z. Guo, M. Wang, L. Chen, Y. Liu, K. G. Zhou, F. Pan and Z. Jiang, *Nat. Commun.*, 2022, **13**, 7123.
58 R. K. Joshi, P. Carbone, F. C. Wang, V. G. Kravets, Y. Su, I. V. Grigorieva, H. A. Wu, A. K. Geim and R. R. Nair, *Science*, 2014, **343**, 752–754.
59 F. Li, J. Zhu, P. Sun, M. Zhang, Z. Li, D. Xu, X. Gong, X. Zou, A. K. Geim, Y. Su and H. M. Cheng, *Nat. Commun.*, 2022, **13**, 4472.